Published in final edited form as:

RSC Adv. 2017 ; 7(84): 53236–53246. doi:10.1039/C7RA09899E.

Anticancer potency of nitric oxide-releasing liposomes

Dakota J. Suchyta and **Mark H. Schoenfisch**

Department of Chemistry, The University of North Carolina at Chapel Hill, Chapel Hill, North Carolina, 27599

Abstract

In this study, fast and slow nitric oxide (NO)-releasing liposomes (half-lives of 2.5 and >72 h, respectively) were prepared by encapsulation of N-propyl-1,3-propanediamine/NO (PAPA/NO) and diethylenetriamine/NO (DETA/NO), respectively, via reverse phase evaporation. The anticancer activity of the otherwise equivalent fast and slow NO-releasing systems was evaluated against several distinct pancreatic, colorectal, and breast cancer cell lines. The anticancer assays (via cytotoxicity) over 72 h revealed that the slower NO-releasing liposomes consistently required lower NO payloads (LD50 <3 μg/mL) relative to the fast NO-release system (LD50 >6 μg/mL) to elicit cytotoxicity. The mechanism of intracellular NO build-up in cancer cells was studied using confocal fluorescence microscopy and flow cytometry, the results of which indicated that a more gradual NO accumulation was characteristic of the slow NO-release system. Protein expression via Western blot analysis revealed that slower NO release resulted in more necrotic/apoptotic cells, while faster release reduced the number of mitotic cells to a greater extent. Overall, these studies demonstrate the potential of NO-releasing liposomes for anticancer therapy and highlight the significance of release kinetics (and NO payloads) required to induce cell death.

Abstract graphic:

Corresponding Author schoenfisch@unc.edu.

Conflicts of interest

The authors declare no competing financial interests.

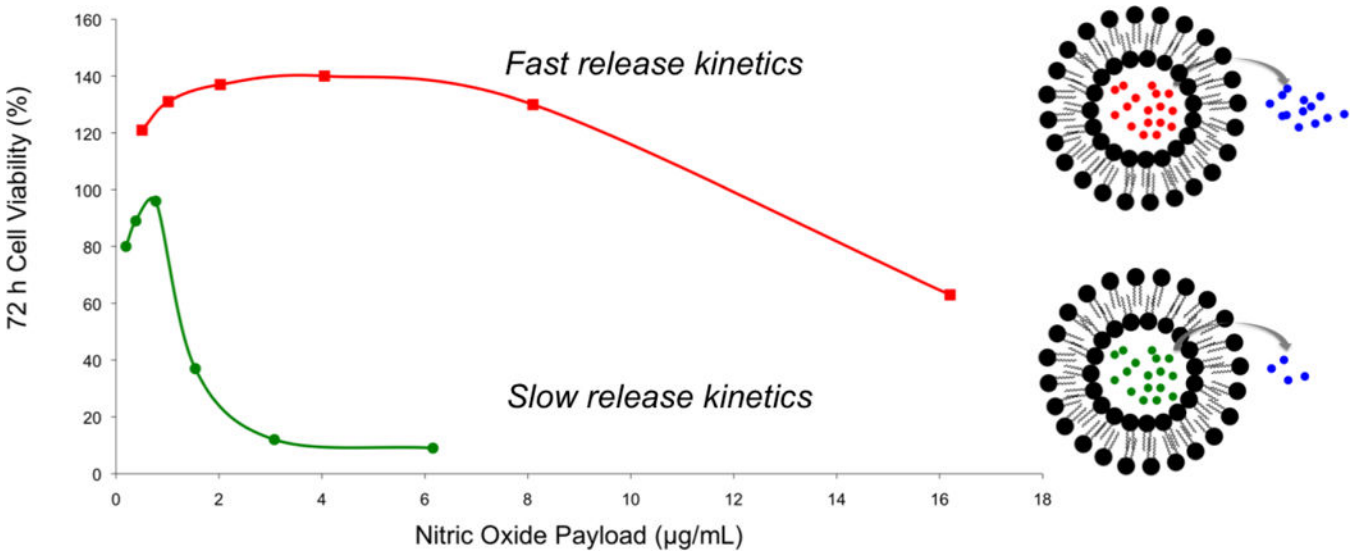

Keywords

Liposome; drug delivery; nitric oxide; cancer; release kinetics; flow cytometry

Introduction

Small molecule chemotherapeutics (e.g., doxorubicin and cisplatin) often exhibit off-target cytotoxicity due to poor localization.[1–5] The use of a large macromolecular (e.g., polymer, nanoparticle) carrier to deliver the therapeutic to the targeted site represents one method for mitigating the adverse side effects of small molecules. The leaky vasculature of tumors allows macromolecules to extravasate at the malignant site, with the delivery of the therapeutic payload via cellular uptake or triggered release (e.g., pH and temperature).[6] Liposomes are among the most widely-investigated delivery systems available for drug delivery. Traditionally, liposomes are composed of an aqueous inner core separated from the external solution by a phospholipid bilayer. This unique architecture allows for the confinement of compounds with a wide range of molecular weights, hydrophobicities, and charges until delivery at a location of interest. The ability of liposomes to absorb and fuse with cell membranes enhances the intracellular uptake of the therapeutic payload, a process that is not typically observed for other macromolecular vehicles (e.g., nanoparticles). Liposomes have thus been developed for a number of therapeutic agents, such as gemcitabine and DNA.[6–7] The exterior surface properties of the liposome (e.g., charge) may be tuned independently of the encapsulant, a critical feature for impacting targeting capabilities and/or reducing aggregation in the bloodstream. In this manner, liposomes have improved the anticancer delivery of many chemotherapeutics, including doxorubicin, arsenic trioxide, and daunorubicin.[8–10]

Nitric oxide (NO), an endogenous diatomic free radical, is an important mediator of inflammation,[11–13] vasodilation,[14–15] biocidal action,[16–18] cardio- and neuroprotection,[19–20] and cancer cell proliferation/killing.[21–23] Off-target toxicity of NO is mitigated by

scavenging and/or reaction to nitrite/nitrate.[14] Nitric oxide donors have been developed as a strategy for delivering NO to biological systems as dissolved NO rather than a gas. Examples of currently approved NO donors include sodium nitroprusside, isosorbide mononitrate, glyceryl trinitrate, and pentaerythrityl tetranitrate.[24] *N*-diazeniumdiolates are a class of NO donors that spontaneously release NO under physiological conditions. The rate of NO release depends on the molecular structure of the amine precursor, facilitating diverse and tunable NO-release kinetics.[25–26] With respect to chemotherapy, the pH-dependent release of *N*-diazeniumdiolates is advantageous because tumor microenvironments are generally more acidic (pH ~6) than healthy tissue (pH 7.4).[27–28] The lower pH promotes accelerated NO release at the tumor. A vast literature has proven that small molecule *N*-diazeniumdiolates are capable of eliciting potent anticancer action.[29–35] Clinical utility has not been achieved because of the excessive loss of NO, prematurely, prior to reaching the tumor site.

In this study, two *N*-diazeniumdiolate-encapsulated liposome systems were prepared with distinct NO-release kinetics (fast and slow). The anticancer activity of these liposomes was evaluated against pancreatic, colorectal, and breast cancer cell lines. Confocal fluorescence and flow cytometry were used to measure both cellular uptake of the liposomes and intracellular NO delivery. The effect of the NO release on protein expression, specifically cleaved PARP, cyclin B1, and cyclin D1, was also examined via Western blot analysis to assess apoptosis and cell cycle arrest/ejection.

Experimental

Materials.

Dipalmitoylphosphatidylcholine (DPPC) and 1,2-dipalmitoyl-*sn*-glycero-3-phosphoethanolamine-N-(lissamine rhoadmine B sulfonyl) ammonium salt (Rh-PE) were purchased from Avanti Polar Lipids (Alabaster, AL). Cholesterol (Chol), paraformaldehyde, propidium iodide, fetal bovine serum (FBS), penicillin streptomycin, 1x Dulbecco's modified Eagle's medium (DMEM), McCoy's 5A medium, RPMI 1640 medium, Dulbecco's phosphate-buffered saline (DPBS) for cell culture, *N*-propyl-1,3-propanediamine (PAPA), and diethylenetriamine (DETA) were obtained from Sigma (St. Louis, MO). Prolong diamond antifade mountant, 4-amino-5-methylamino-2',7'-difluorofluorescein diacetate (DAF-FM), trypsin, Accutase, Annexin V Pacific Blue conjugate, 1% (v/v) NP40 lysis buffer, chloroform, phenazine methosulfate (PMS), anhydrous acetonitrile, anhydrous diethyl ether, dimethyl sulfoxide (DMSO), anhydrous ethanol (EtOH), sulfuric acid (H_2SO_4), protein stripping buffer, sodium hydroxide (NaOH), calcium chloride ($CaCl_2$), PageRuler Plus prestained protein ladder, and secondary antibodies (both mouse and rabbit) for Western blotting were purchased from Fisher Scientific (Fair Lawn, NJ). Sephadex G-25 was obtained from GE Healthcare (Pittsburgh, PA). 3-(4,5-dimethylthiazol-2-yl)-5-(3-carboxymethoxyphenyl)-2-(4-sulfophen-yl)-2H-tetrazolium inner salt (MTS) was purchased from Promega (Madison, WI). Primary antibodies for total and cleaved PARP (rabbit), cyclin B1 (rabbit), cyclin D1 (rabbit), and vinculin (mouse) used in Western blotting were obtained from Cell Signaling (Danvers, MA). Western lightning ECL pro substrate for Western blot detection was from PerkinElmer (Waltham, MA). Phosphatase and protease

inhibitors were purchased from Roche (Basel, Switzerland). Criterion TGX Gel, tris/glycine transfer buffer with sodium dodecyl sulfate (SDS), tris-buffered saline with Tween 20 (TBST), and polyvinylidene fluoride (PVDF) transfer membrane were obtained from Bio-Rad (Hercules, CA). Nitric oxide (NO; 99.5%), nitrogen (N_2; 99.998%), argon (Ar; 99.995%), and NO calibration (26.80 ppm, balance N_2) gases were obtained from Airgas National Welders (Durham, NC). A Millipore Milli-Q UV Gradient A10 System (Bedford, MA) was used to purify distilled water to a resistivity of 18.2 MΩ·cm and a total organic content ≤6 ppb. MIA PaCa-2, AsPc1, and Pa14c pancreatic cancer cells were a gift from Dr. Channing Der of the Department of Pharmacology at the University of North Carolina (Chapel Hill, NC). MDA-MB-231, MCF-7, MDA-MB-468, HCT116, HT-29, and SW480 breast and colorectal cancer cells were a gift from Dr. Matthew Lockett of the Department of Chemistry at the University of North Carolina (Chapel Hill, NC).

Synthesis of N-diazeniumdiolate NO donors.

A previously reported method was used to synthesize small molecule *N*-diazeniumdiolate NO donors.[27] Briefly, DETA and PAPA were dissolved in anhydrous acetonitrile at a concentration of 33.3 mg/mL. The solution was then purged with Ar to 100 psi inside a stainless steel Parr bomb. Six consecutive purges with Ar (three quick purges of 10 s each, followed by three slow purges of 10 min each) were carried out to remove dissolved oxygen. The solution was subsequently pressurized to 145 psi with NO for 3 d, after which the solution was purged again with Ar (100 psi) at least six times to remove residual NO. The precipitated product was filtered over a Hirsch funnel, washed three times with diethyl ether, and dried under vacuum overnight. The final NO donor product was stored at −20°C until use.

Liposome synthesis.

The liposomes were prepared using a reverse phase evaporation method.[37] A 1:1 molar ratio of lipid to Chol (49.5 μmol lipid:49.5 μmol Chol) was dissolved in a mixture of diethyl ether (5.0 mL) and chloroform (5.0 mL) in a round-bottom flask under N_2 atmosphere. Fluorescent liposomes were prepared using the above protocol, but with 1 mol% lipid of Rh-PE. The *N*-diazeniumdiolate was dissolved in 10 mM NaOH to make a 14 mM stock NO donor solution. This solution was injected into the flask, and then sonicated for 4 min at 45°C. The organic phase was removed by rotoevaporation to yield the aqueous liposome suspension. Liposomes were incubated at 45°C for an additional 30 min, after which the unencapsulated material was removed using four Sephadex G-25 spin columns packed in 10-mL syringes. The liposomes collected from the column were stored at 4°C.

Characterization of liposomes.

Dynamic light scattering (DLS; Malvern Zetasizer Nano; UK) was used to determine liposome size distribution in water. Transmission electron microscopy (TEM) was used to confirm liposome formation. Liposome samples for TEM analysis were prepared by diluting the stock solution with Milli-Q water (1:1 volumetric ratio) and casting the suspension onto Formvar-coated, square mesh copper TEM grids (Electron Microscopy Sciences, Hatfield, PA). The solvent was allowed to evaporate for 45 min prior to applying a negative-stain using a 2% (w/v) uranyl acetate solution. A drop of the stain was left on the grid for 30 s and

then removed using filter paper. The grid was dried for 5 min prior to imaging using a JEOL 100CX II transmission electron microscope (100 kV accelerating voltage).

Nitric oxide release.

Nitric oxide storage and NO-release kinetics from the liposomes were measured using a Sievers Chemiluminescence Nitric Oxide Analyzer (NOA; Boulder, CO).[38–39] Studies to evaluate NO-release kinetics were performed in 10 mM PBS (pH 7.4) at 37°C. The instrument was calibrated using air passed through a NO zero filter (0 ppm NO) and a 26.80 ppm NO standard (balance N_2). Nitric oxide storage for encapsulation efficiency (i.e., the extent to which the NO donor is entrapped within the liposomal aqueous core) was performed in a 2:1 volumetric ratio of ethanol to 0.183 M sulfuric acid (30 mL total volume) at 37°C. The encapsulation efficiency was calculated by comparing the liposome NO storage to the amount of NO in the free donor solution used during liposome preparation. All presented data is from $n \geq 3$ separate liposome preparations. Nitric oxide release measurements were terminated when the NO concentration dropped below 10 ppb per 300 μL liposomes.

Cytotoxicity assays.

Pa14c and MIA PaCa-2 cells were cultured in DMEM. HCT116 and HT-29 cells were cultured in McCoy's 5A medium. MDA-MB-231, MCF-7, MDA-MB-468, SW480, and AsPc1 cells were cultured in RPMI medium. All media were supplemented with 10 vol% FBS and 1 wt% penicillin/streptomycin. Cells were maintained at 37°C in a humidified incubator with 5 vol% CO_2. For cell viability evaluations, the MTS assay was used as previously described with cells plated in triplicate.[40] Briefly, cells (2×10^3 cells/well) in DMEM were treated with various volumes of liposomes in a 96-well plate (100 μL total volume per well). Following a 72 h incubation period at 37°C, the supernatant of each well was removed, rinsed with PBS (100 μL), and replaced with fresh DMEM (100 μL). The cells were further incubated with 20 μL of MTS/PMS reagent (20:1 v/v MTS to PMS) at 37°C for ~90 min. The absorbances of the resulting solutions at 490 nm were measured using a Thermoscientific Multiskan EX plate reader (Waltham, MA). The ratio of absorbance values between the samples and the controls was represented as the percent cell viability. Dose response curves and LD_{50} values were plotted and tabulated using GraphPad Prism 6 software (La Jolla, CA) and non-linear regression (three- parametric Hill function), respectively. All presented data are from $n \geq 3$ separate experiments.

Confocal fluorescence microscopy.

Cells were plated in 10×10 mm cloning cylinders (VWR, Atlanta, GA) secured to No 1.5 glass cover slips (VWR, Atlanta, GA) using silicone grease. The slip was placed in a Petri dish prior to the addition of cell media. After 24 h, the medium within the cylinders was replaced with a 10 μM DAF-FM solution. An additional 30 min incubation period at 37°C was then carried out before removing the DAF-FM solution. Fresh cell media was subsequently added and allowed to incubate for another 15 min at 37°C to allow for saponification of the probe. Liposomes were added to the cells and incubated for 2 h, followed by rinsing twice with 100 μL DPBS. A 100-μL aliquot of 4 vol% paraformaldehyde solution (diluted with DPBS) was injected into the wells and incubated

for 15 min at room temperature. The cover slips were then mounted on glass slides using a droplet of mounting media, sealed with nail polish (Electron Microscopy Sciences; Hatfield, PA), and imaged after 1 h using a Zeiss LSM 700 laser scanning confocal microscope. The excitation/emission wavelengths for DAF-FM and Rh-PE were 495/515 and 560/583 nm, respectively. Fiji software was used for image processing and densitometry calculations. Autoquant X3 software (Media Cybernetics; Warrendale, PA) generated orthogonal views of the z-stacked images. All images were collected under cosntant exposure times. The images were also processed equivalently and normalized to a single brightness level.

Flow cytometry.

Cells were plated (1×10^4 cells/well) in 96-well plates and allowed to adhere for 24 h in RPMI media (100 μL). The media was then removed and cells were incubated with fresh media containing 5 μM DAF-FM for 1 h. The media containing the DAF-FM was subsequently removed and free or liposomal *N*-diazeniumdiolate NO donors were added to the wells (dissolved in fresh media) and allowed to incubate for specified times. Cells were then washed with DPBS and detached by exposure to Accutase (30 μL) for 5 min at room temperature. Media containing 5 mM $CaCl_2$ was added (30 μL) to the wells while maintaining the plate at 0°C for 20 min. Annexin V (4 μL) and propidium iodide (3 μL from a 3 μg/mL stock solution) were added to the wells for cell staining. The plate was placed on a shaker for 30 s (2000 rpm) to resuspend cells prior to analysis with an iQue Screener Plus flow cytometer (IntelliCyt, Albuquerque, NM). A 33 s sampling (sip) time was used with a 0.5 s up time between wells. The plate was shaken (and the probe cleaned) for 20 s at 2000 rpm every 4 wells. Data acquisition and processing were carried out with ForeCyt software (IntelliCyt; Albuquerque, NM). Single color compensation controls were performed to minimize spectral overlap. Gates were placed around singlet cells to exclude data from aggregated cells. Fluorescence intensities were calculated and plotted versus number of events.

Western blot analysis.

Cells were added to a 6-well plate (3×10^5 cells/well) and incubated for 24 h. Media was then removed and replaced with fresh media containing liposomes. At specified timepoints, the plates were placed on ice, washed once with cold DPBS, and incubated for 15 min with 1 vol% NP40 lysis buffer (50 μL) containing protease and phosphatase inhibitors. The wells were then scraped and the solution added to cold microcentrifuge tubes. Cellular debris was removed by centrifugation (4°C, 5 min). Protein concentrations in samples were determined using the Bradford assay. Equal total protein amounts (~30 μg) were added to each lane of the gel (4–20% gradient). After electrophoresis, the proteins were transferred onto PVDF membranes, blocked with 5% (w/v) milk, and stained with primary antibody overnight. After incubation with the secondary antibody for 1 h, the membrane was incubated with the Western lightning ECL pro substrate (10 min) and then imaged using a ChemiDoc chemiluminescence imaging system (Bio-Rad; Hercules, CA). Western blot images were processed using Image Lab software (Bio-Rad; Hercules, CA). Fiji software was used for densitometry calculations. Loading controls were used as a normalization factor for densitometric calculations.

Results and Discussion

The *N*-diazeniumdiolates used in this study (PAPA/NO and DETA/NO; Figure S1) were selected because of their dissimilar NO-release half-lives in PBS at pH 7.4 (0.25 h and 20 h, respectively). On the basis of our previous work and that of others,[28,41] we hypothesized that the resulting NO-releasing liposomes would have different NO-release kinetics. Liposome formation was confirmed by dynamic light scattering (DLS) measurements. As shown in Figure 1, DETA/NO and PAPA/NO liposomes exhibited hydrodynamic sizes typical of liposomes synthesized via reverse-phase evaporation (Table 1).[37] The slight difference in size between the systems should not appreciably affect their anticancer activity as liposomes with sizes of approximately 150 to 400 nm exhibit similar cellular uptake.[42] Transmission electron microscopy (TEM) corroborated the DLS measurements and indicated negligible liposome-liposome fusion (Figure S2). Real-time NO release measurements demonstrated that the NO donor encapsulation efficiency was similar to efficiencies of other reverse-phase evaporated liposomes and consistent between the two liposome formulations (Table 1), likely the result of similar size of the NO donors.[37] As expected, the liposomes released NO more slowly at physiological pH (7.4) than the corresponding small molecule NO donor alone (Figure 1). The PAPA/NO liposomes released ~50% of their total NO in 2.5 h, a ten-fold longer NO-release half-life than the free NO donor. As the rate of NO release impacts NO's toxicity,[29–35] the use of two distinct *N*-diazeniumdiolates as encapsulants allows for the study of the anticancer therapeutic potential of the liposomes as a function of NO-release kinetics.

Cytotoxicity of the liposomes.

The potential anticancer activity of the NO-releasing liposomes was initially tested against Pa14c pancreatic cancer cells, an aggressive pancreatic cancer cell line. The PAPA/NO and DETA/NO liposome systems showed a pronounced toxicity difference, attributable to the NO release (Figure 2A). At low NO payloads (~0.9 μg/mL), the viability was slightly enhanced for each liposomal system. Previous research has reported that low levels of NO induces EGF-dependent cell proliferation.[14,43] At NO payloads >1.5 μg/mL, the slower NO-release system (DETA/NO liposomes) was markedly more toxic towards the Pa14c cells. The less effective PAPA/NO liposomes required larger NO payloads to induce toxicity likely because of the faster release rate, resulting in the release of the majority of the NO payload before reaching the cell and/or cellular uptake. Significantly less toxicity (killing) was observed (Figure S3) when using a noncancerous epithelial cell line (HPNE), indicating that NO may elicit greater cytotoxicity towards cancer cells by further enhancing the existing oxidative and nitrosative stresses that such cells are already experiencing.[44]

The cytotoxicity of the liposomes was next evaluated against a number of malignant lines from pancreatic, breast, and colorectal cancers to ascertain if the observed dependence on NO-release kinetics applied to other cell lines. The slow NO-releasing liposomes (DETA/NO) consistently required lower NO payloads to elicit cytotoxic effects, regardless of cancer type or cell line (Figure 2B). In fact, the LD_{50} was <3 μg/mL NO for the DETA/NO liposomes against all cancer cell lines investigated, while the faster-releasing PAPA/NO liposomes required >6 μg/mL NO to elicit cytotoxic action. These results agree

with prior work that demonstrated that free NO donors exhibiting slow NO-release kinetics required lower anticancer payloads relative to their fast-releasing counterparts.[29,33,45]

A human breast cancer cell line (MCF-7) was chosen as a representative model for further evaluation of the NO-release kinetics and associated cytotoxicity because of the stark differences in the LD_{50} values for the PAPA/NO and DETA/NO liposomes. Our immediate goal was to determine if the PAPA/NO liposomes induced cytotoxicity earlier in the assay (i.e., before 72 h). Cells were exposed to the 72 h LD_{50} concentrations of the DETA/NO and PAPA/NO liposomes (0.75 μg/mL and 16.2 μg/mL after 72 h exposure, respectively) for 8, 24, 48, and 72 h. As shown in Figure 3, neither the fast nor slow NO-releasing liposome system exhibited cytotoxic effects at early timepoints (8 h). Rather, mild cell proliferation was noted for both. After 24 h, cell viability diminished greatly (up to 60%) for cells exposed to the PAPA/NO system (16.2 μg/mL NO), with no further change through 72 h. PAPA/NO liposomes deliver ~90% of the NO payload by 24 h (Figure 1), correlating with this observed cytotoxicity. The NO liberated from the DETA/NO liposomes (0.75 μg/mL) displayed a more consistent cell viability profile with a steady drop over the 72 h period. Cytotoxicity for PAPA/NO liposomes at 0.75 μg/mL payloads was not induced at any time point (negligible toxicity relative to controls). Collectively, this data suggests that faster NO release (i.e., using shorter half-life NO donors) elicits cytotoxicity more rapidly than corresponding slower release, but necessitates larger NO payloads. Relative to the slower NO-releasing liposomes, the greater levels of NO from the fast release liposomes may work to increase the entropy within the cells through protein denaturation.

Intracellular liposome uptake and NO delivery.

The observed relationship between liposome NO-release kinetics and anticancer action was hypothesized to be the result of intracellular NO accumulation. Confocal fluorescence microscopy was employed to measure intracellular NO build-up over time for the two systems using DAF-FM, a molecular probe that selectively reacts with NO to form a fluorescent benotriazole compound.[46] Additionally, cellular uptake of the liposomes was visualized by incorporating a fluorescent phospholipid (Rh-PE) into the lipid bilayer.[47] A 2 h exposure period was initially selected for this study as cell have been shown to initiate liposomal uptake within this timeframe,[48–49] allowing for visualization of delivered NO. The bright field and fluorescence images of MCF-7 cells after exposure to DETA/NO and PAPA/NO liposomes (at their LD_{50} values) are provided in Figure 4A. Of note, the amount of NO released during the confocal experiment is significantly lower than the corresponding LD_{50} values due to the shorter exposure time (2 vs. 72 h). Liposome uptake was clearly observed after 2 h, with z-stack images revealing intracellular localization of the NO-releasing liposomes (Figure 5). The rapid uptake of the liposomes results from their ability to adsorb to and then fuse with the cell membrane, a phenomenon that does not readily occur with other delivery vehicles (e.g., nanoparticles).[6] Relative to DETA/NO liposomes, cells exposed to PAPA/NO liposomes had substantially elevated levels of intracellular NO. Densitometry calculations were carried out to quantify intracellular NO levels for the two liposomes (Figure 4B). Treatment with PAPA/NO liposomes resulted in a 4-times larger fluorescence signal relative to DETA/NO after 2 h, supporting the results observed in the time-course study where the fast release system elicited more rapid cytotoxicity (at 24 h).

The lack of cytotoxicity observed for the PAPA/NO liposomes at the same NO payloads as the DETA/NO liposomes (0.75 μg/mL) was supported by negligible intracellular NO accumulation at 2 h (data not shown). Collectively, the greater NO accumulation and NO exposure observed for the PAPA/NO liposomes leads to more rapid anticancer action.

Kinetics of intracellular NO accumulation.

The rapid NO delivery from the PAPA/NO liposomes was hypothesized to be key in eliciting cytotoxicity at short time periods (i.e., 24 h).The more gradual cell killing observed using the DETA/NO liposomes would be expected to parallel the build-up of intracellular NO over time. Flow cytometry was utilized to quantify NO accumulation within the MCF-7 cells over a 72-h period using the same DAF-FM probe (Figure 6). A large increase in intracellular fluorescence was observed by 24 h for cells treated with PAPA/NO liposomes (16.2 μg/mL NO). At 48 and 72 h, the fluorescence essentially remained at the same level, signaling that no more NO was delivered to the cell. In contrast, the fluorescence within cells treated with the slower NO-releasing DETA/NO liposomes (0.75 μg/mL NO) continued to increase steadily over the entire 72 h period. The therapeutic action of both slow and fast NO-releasing liposomes followed the same trend observed in the cytotoxicity time-course study, where cytotoxicity was elicited more rapidly with PAPA/NO liposomes and the DETA/NO liposomes required the full 72 h before eliciting toxicity. At equal NO payloads (0.75 μg/mL), minimal intracellular NO accumulation was observed for the PAPA/NO liposomes due to premature NO loss prior to cellular uptake (Figure S4), which is in agreement with cytotoxicity findings.

A median fluorescence intensity comparison between free and liposomal NO donors was performed to highlight the benefits of using NO-releasing liposomes over the low molecular weight NO donors. Cells treated with NO-releasing liposomes exhibited greater intracellular NO accumulation (Figure 6), as a result of enhanced NO donor stability (within the liposomes) and targeted cellular uptake. Similar behavior has been observed for other small molecule drugs (e.g., gemcitabine and doxorubicin) encapsulated within liposomes.[8,50]

Effect of NO-releasing liposomes on intracellular signaling.

Flow cytometry studies analyzing the number of apoptotic and necrotic cells after treatment with the NO-releasing liposomes were carried out to provide information on the cell killing mechanism. Cells that stained positive for propidium iodide (PI) but negative for Annexin V were considered necrotic; those stained negative for PI but positive for Annexin V were early apoptotic; and, cells that stained positive for both markers were considered late apoptotic.[51] As shown in Figure 7, cancer cells treated with PAPA/NO liposomes (16.2 μg/mL NO) resulted in similar populations of early apoptotic, late apoptotic, and necrotic cells. In contrast, DETA/NO liposomes (0.75 μg/mL NO) yielded more necrotic and early apoptotic cells. These results paralleled prior research that observed greater necrosis and apoptosis for leukemia cells treated with DETA/NO versus PAPA/NO.[45]

The flow cytometry data was supplemented with Western blot analysis to evaluate if any differences existed in protein expression levels. Poly(ADP-ribose) polymerase (PARP) is a critical mediator of DNA repair and upon cleavage by caspase-3 initiates cellular breakdown

and apoptosis.[52] A measurement of increased PARP levels after treatment would indicate that cells underwent PARP-mediated apoptosis. Cyclin analysis would facilitate understanding the cell cycle and whether cells were arrested or ejected.[53–54] The expressions of these regulator proteins in MCF-7 cells were measured after NO exposure at 24, 48, and 72 h (Figure 8A). Cleaved PARP levels were the greatest for cells treated with 16.2 μg/mL NO from PAPA/NO liposomes, indicating apoptosis, especially at early timepoints (i.e., 24 and 48 h). This data correlates well with the rapid cytotoxicity observed from the fast NO-release system (Figure 3). Densitometric calculations were performed on the blots to more accurately compare protein levels between exposure conditions. Even though cells treated with DETA/NO liposomes exhibited reduced cyclin B1 levels relative to controls by 24 h (Figure 8B), the levels were still greater than cells treated with PAPA/NO liposomes. At 72 h, the two systems, at their respective LD_{50} values, had similar expressions of cyclin D1 (Figure 8C), suggesting an equivalent capacity to either inactivate transcription factors that drive cell proliferation (i.e., prevent cell growth) or initiate cyclin D1 destruction. Of note, minimal changes in protein expression were observed for cells exposed to PAPA/NO liposomes at NO payloads (0.75 μg/mL) equivalent to the DETA/NO liposomes, corroborating insufficient NO delivery and low toxicity. These results suggest that both types of NO-releasing liposomes trigger the same anticancer pathways, but to different degrees depending on the exposure time and NO concentration. Slower NO release elicits a more gradual increase in cleaved PARP levels (i.e., apoptosis) and arrested cells in the cell cycle, while faster NO release promotes rapid PARP cleavage and prevention of mitosis.

Conclusions

The transition from low molecular weight NO donors to macromolecular NO-release systems for anticancer treatments may represent an important step in creating more effective chemotherapies. Two NO-releasing liposome systems with distinct NO-release kinetics were used to study cytotoxicity against pancreatic, colorectal, and breast cancer cell lines. Through the encapsulation of the low molecular weight NO donors within liposomes, greater intracellular NO accumulation was observed due to enhanced uptake. The preliminary cell studies herein suggest that NO-release kinetics play an important role in eliciting cell death, with a direct relationship to intracellular NO accumulation. Fast NO-releasing liposomes represent a less effective anticancer therapeutic as the NO is liberated too rapidly in advance of intracellular uptake. The ability of NO to further increase the oxidative/nitrosative stresses that cancer cells expereince is a unique mechanism to enhance killing action on cancer cells over healthy cells. Future studies will evaluate the benefits of targeting ligands (e.g. folate) on directing the NO-releasing liposomes to tumors.

Supplementary Material

Refer to Web version on PubMed Central for supplementary material.

Acknowledgements

Funding for this research was provided by the National Institutes of Health (DE025207). This work was performed in part at the Chapel Hill Analytical and Nanofabrication Laboratory (CHANL), a member of the North Carolina Research Triangle Nanotechnology Network (RTNN), which is supported by the National Science Foundation,

Grant ECCS-1542015, as part of the National Nanotechnology Coordinated Infrastructure (NNCI). The UNC Flow Cytometry Core Facility is supported in part by P30 CA016086 Cancer Center Core Support Grant to the UNC Lineberger Comprehensive Cancer Center. The Intellicyt iQue Screener PLUS is supported in part by the North Carolina Biotech Cancer Institutional Support Grant 2015-IDG-1001. We would like to thank Dr. Pablo Ariel for his guidance in analyzing the confocal fluorescence microscopy images, Sébastien Coquery for help with the collection and processing of the flow cytometry data, and Samuel George and Nathan Whitman for their assistance in the Western blot experiments.

References

(1). Bender A; Schieber J; Glick M; Davies JW; Azzaoui K; Hamon J; Urban L; Whitebread S; Jenkins JL Analysis of pharmacology data and the prediction of adverse drug reactions and off-target effects from chemical structure. ChemMedChem, 2007, 2, 861–873. [PubMed: 17477341]

(2). Park BK; Boobis A; Clarke S; Goldring C; Jones D; Kenna JG; Lambert C; Laverty HG; Naisbitt DJ; Nelson S; Nicoll-Griffith DA; Obach RS; Routledge P; Smith DA; Tweedie DJ; Vermeulen N; Williams DP; Wilson ID; Baillie TA Managing the challenge of chemically reactive metabolites in drug development. Nature Reviews Drug Discovery, 2011, 10, 292–306. [PubMed: 21455238]

(3). Widakowich C; De Castro G; De Azambuja E; Dinh P; Awada A Review: Side effects of approved molecular targeted therapies in solid cancers. The Oncologist, 2007, 12, 1443–1455. [PubMed: 18165622]

(4). Galluzzi L; Vitale I; Michels J; Brenner C; Szabadkai G; Harei-Bellan A; Castedo M; Kroemer G Systems biology of cisplatin resistance: Past, present and future. Cell Death and Disease, 2014, 5, 1–18.

(5). De Angelis A; Urbanek K; Cappetta D; Piegari E; Ciuffreda L; Rivellino A; Russo R; Esposito G; Rossi F; Berrino L Doxorubicin cardiotoxicity and target cells: A broader perspective. Cardio-Oncology, 2016, 2, 1–8. [PubMed: 28133540]

(6). Torchilin VP Recent advances with liposomes as pharmaceutical carriers. Nature Reviews Drug Discovery, 2005, 4, 145–160. [PubMed: 15688077]

(7). Allen TM; Cullis PR Liposomal drug delivery systems: From concept to clinical applications. Advanced Drug Delivery Reviews, 2013, 65, 36–48. [PubMed: 23036225]

(8). Barenholz YC Doxil – The first FDA-approved nano-drug: Lessons learned. Journal of Controlled Release, 2012, 160, 117–134. [PubMed: 22484195]

(9). Chen H; MacDonald RC; Li S; Krett NL; Rosen ST; O'Halloran TV Lipid encapsulation of arsenic trioxide attenuates cytotoxicity and allows for controlled anticancer drug release. Journal of the American Chemical Society, 2006, 128, 13348–13349. [PubMed: 17031934]

(10). Piccaluga PP; Visani G; Martinelli G; Isidori A; Malagola M; Rondoni M; Baccarani M; Tura S Liposomal daunorubicin (daunoXome) Liposomal daunorubicin (daunoXome) for treatment of relapsed meningeal acute myeloid leukemia. Leukemia, 2002, 16, 1880–1881. [PubMed: 12200714]

(11). Taylor EL; Megson IL; Haslett C; Rossi AG Nitric oxide: A key regulator of myeloid inflammatory cell apoptosis. Cell Death and Differentiation, 2003, 10, 418–430. [PubMed: 12719719]

(12). Wink DA; Hines HB; Cheng RS; Switzer CH; Flores-Santana W; Vitek MP; Ridnour LA; Colton CA Nitric oxide and redox mechanisms in the immune response. Journal of Leukocyte Biology, 2011, 89, 873–891. [PubMed: 21233414]

(13). Sharma JN; Al-Omran A; Parvathy SS Role of nitric oxide in inflammatory diseases. Inflammopharmacology, 2007, 15, 252–259. [PubMed: 18236016]

(14). Thomas DD; Ridnour LA; Isenberg JS; Flores-Santana W; Switzer CH; Donzelli S; Hussain P; Vecoli C; Paolocci N; Ambs S; Colton CA; Harris CC; Roberts DD; Wink DA The chemical biology of nitric oxide: Implications in cellular signaling. Free Radical Biology & Medicine, 2008, 45, 18–31. [PubMed: 18439435]

(15). Moncada S; Palmer R; Higgs E Nitric oxide: Physiology, pathophysiology, and pharmacology. Pharmacological Reviews, 1991, 43, 109–142. [PubMed: 1852778]

(16). Carpenter AW; Schoenfisch MH Nitric oxide release: Part II. Therapeutic applications. Chemical Society Reviews, 2011, 41, 3742–3752.

(17). Fang FC Perspective series: Host/pathogen interactions. Mechanisms of nitric oxide-related antimicrobial activity. Journal of Clinical Investigation, 1997, 99, 2818–2825. [PubMed: 9185502]

(18). Fang FC Antimicrobial reactive oxygen and nitrogen species: Concepts and controversies. Nature Reviews Microbiology, 2004, 2, 820–832. [PubMed: 15378046]

(19). Jones SP; Bolli R The ubiquitous role of nitric oxide in cardioprotection. Journal of Molecular and Cellular Cardiology, 2006, 40, 16–23. [PubMed: 16288777]

(20). Calabrese V; Mancuso C; Calvani M; Rizzarelli E; Butterfield DA; Stella AM Nitric oxide in the central nervous system: Neuroprotection versus neurotoxicity. Nature Reviews Neuroscience, 2007, 8, 766–775. [PubMed: 17882254]

(21). Wink DA; Vodovotz Y; Laval J; Laval F; Dewhirst MW; Mitchell JB The multifaceted roles of nitric oxide in cancer. Carcinogenesis, 1998, 19, 711–721. [PubMed: 9635855]

(22). Wang L; Xie K Nitric oxide and pancreatic cancer pathogenesis, prevention, and treatment. Current Pharmaceutical Design, 2010, 16, 421–427. [PubMed: 20236070]

(23). Sullivan R; Graham CH Chemosensitization of cancer by nitric oxide. Current Pharmaceutical Design, 2008, 14, 1113–1123. [PubMed: 18473858]

(24). Miller MR; Megson IL Recent developments in nitric oxide donor drugs. British Journal of Pharmacology, 2007, 151, 305–321. [PubMed: 17401442]

(25). Hrabie JA; Klose JR; Wink DA; Keefer LK New nitric oxide-releasing zwitterions derived from polyamines. Journal of Organic Chemistry, 1993, 58, 1472–1476.

(26). Keefer LK Fifty years of diazeniumdiolate research. From laboratory curiosity to broad-spectrum biomedical advances. ACS Chemical Biology, 2011, 6, 1147–1155. [PubMed: 21932836]

(27). Shamim U; Hanif S; Albanyan A; Beck F; Bao B; Wang Z; Banerjee S; Sarkar FH; Mohammad RM; Hadi SM; Azmi AS Resveratrol-induced apoptosis is enhanced in low pH environments associated with cancer. Journal of Cellular Physiology, 2012, 227, 1493–1500. [PubMed: 21678400]

(28). Tannock IF; Rotin D Acid pH in tumors and its potential for therapeutic exploitation. Cancer Research, 1989, 49, 4373–4384. [PubMed: 2545340]

(29). Maragos CM; Wang JM; Hrabie JA; Oppenheim JJ; Keefer LK Nitric oxide/nucleophile complexes inhibit the *in vitro* proliferation of A375 melanoma cells via nitric oxide release. Cancer Research, 1993, 53, 564–568. [PubMed: 8425188]

(30). Stuehr DJ; Nathan CF A macrophage product responsible for cytostasis and respiratory inhibition of tumor target cells. Journal of Experimental Medicine, 1989, 169, 1543–1555. [PubMed: 2497225]

(31). Tamir S; Lewis RS; Walker T; Deen WM; Wishnok JS; Tannenbaum SR The influence of delivery rate on the chemistry and biological effects of nitric oxide. Chemical Research in Toxicology, 1993, 6, 895–899. [PubMed: 8117930]

(32). Mooradian DL; Hutsell TC; Keefer LK Nitric oxide (NO) donor molecules: Effect of NO release rate on vascular smooth muscle cell proliferation in vitro. Journal of Cardiovascular Pharmacology, 1995, 25, 674–678. [PubMed: 7596138]

(33). Kielbik M; Klink M; Brzezinska M; Szulc I; Sulowska Z Nitric oxide donors: Spermine/NO and diethylenetriamine induce ovarian cancer cell death and affect STAT3 and AKT signaling proteins. Nitric Oxide, 2013, 35, 93–109. [PubMed: 24055735]

(34). Taylor EL; Megson IL; Haslett C; Rossi AG Dissociation of DNA fragmentation from other hallmarks of apoptosis in nitric oxide-treated neutrophils: Differences between individual nitric oxide donor drugs. Biochemical and Biophysical Research Communications, 2001, 289, 1229–1236. [PubMed: 11741325]

(35). Meßmer UK; Brüne B Nitric oxide (NO) in apoptotic versus necrotic RAW 264.7 macrophage cell death: The role of NO-donor exposure, NAD+ content, and p53 accumulation. Archives of Biochemistry and Biophysics, 1996, 327, 1–10. [PubMed: 8615678]

(36). Suchyta DJ; Schoenfisch MH Encapsulation of *N*-diazeniumdiolates within liposomes for enhanced nitric oxide donor stability and delivery. Molecular Pharmaceutics, 2015, 12, 3569–3574. [PubMed: 26287799]

(37). Szoka F, Jr.; Papahadjopoulos D Procedure for preparation of liposomes with large internal aqueous space and high capture by reverse-phase evaporation. Proceedings of the National Academy of Sciences, 1978, 75, 4194–4198.

(38). Soto RJ; Yang L; Schoenfisch MH Functionalized mesoporous silica via an aminosilane surfactant ion exchange reaction: Controlled scaffold design and nitric oxide release. ACS Applied Materials and Interfaces, 2016, 8,2220–2231. [PubMed: 26717238]

(39). Worley BV; Schilly KM; Schoenfisch MH Anti-biofilm efficacy of dual-action nitric oxide-releasing alkyl chain modified poly(amidoamine) dendrimers. Molecular Pharmaceutics, 2015, 12, 1573–1583. [PubMed: 25873449]

(40). Ganguly S; Bandyopadhyay S; Sarkar A; Chatterjee M Development of a semi-automated colorimetric assay for screening of anti-leishmanial agents. Journal of Microbiological Methods, 2006, 66, 79–86. [PubMed: 16316700]

(41). Elnaggar MA; Subbiah R; Han DK; Joung YK Lipid-based carriers for controlled delivery of nitric oxide. Expert Opinion on Drug Delivery, 2017, 1–13.

(42). Ong S; Ming LC; Lee KS; Yuen KH Influence of the encapsulation efficiency and size of liposomes on the oral bioavailability of griseofulvin-loaded liposomes. Pharmaceutics, 2016, 8, 25.

(43). Villalobo A Nitric oxide and cell proliferation. FEBS Journal, 2006, 273, 2329–2344. [PubMed: 16704409]

(44). Pelicano H; Carney D; Huang P ROS stress in cancer cells and therapeutic implications. Drug Resistance Updates, 2004, 7, 91–110.

45). Shami PJ; Sauls DL; Weinberg JB Schedule and concentration-dependent induction of apoptosis in leukemia cells by nitric oxide. Leukemia, 1998, 12, 1461–1466. [PubMed: 9737697]

(46). Sheng J; Wang D; Braun AP DAF-FM (4-amino-5-methylamino-2',7'-difluorescein) diacetate detects impairment of agonist-stimulated nitric oxide synthesis by elevated glucose in human vascular endothelial cells: Reversal by vitamin C and L-sepiapterin. Journal of Pharmacology and Experimental Therapeutics, 2005, 315, 931–940. [PubMed: 16093274]

(47). Skalko N; Peschka R; Altenschmidt U; Lung A; Schubert R pH-sensitive liposomes for receptor-mediated delivery to chicken hepatoma (LMH) cells. FEBS Letters, 1998, 434, 351–356. [PubMed: 9742953]

(48). Mastrobattista E; Storm G; van Bloois L; Reszka R; Bloemen P; Crommelin DP; Cellular uptake of liposomes targeted to intercellular adhesion molecule-1 (ICAM-1) on bronchial epithelial cells. Biochimica et Biophysica Acta, 1999, 1419, 353–363. [PubMed: 10407086]

(49). Thurston G; McLean JW; Rizen M; Baluk P; Haskell A; Murphy TJ; Hanahan D; McDonald DM Cationic liposomes target angiogenic endothelial cells in tumors and chronic inflammation in mice. Journal of Clinical Investigation, 1998, 101, 1401–1413. [PubMed: 9525983]

(50). Cosco D; Bulotta A; Ventura M; Celia C; Calimeri T; Perri G; Paolino D; Costa N; Veri P; Tagliaferri P; Tassonem P; Fresta M In vivo activity of gemcitabine-loaded PEGylated small unilamellar liposomes against pancreatic cancer. Cancer Chemotherapy and Pharmacology, 2009, 64, 1009–1020. [PubMed: 19263052]

(51). Mishra CB; Mongre RK; Kumari S; Jeong DK; Tiwari M Synthesis, *in vitro* and *in vivo* anticancer activity of novel 1-(4-imino-1-substituted-1*H*-pyrazolo[3,4-*d*]pyrimidin-5(4*H*)-yl)urea derivatives. RSC Advances, 2016, 6, 24491–24500.

(52). Javle M; Curtin NJ The role of PARP in DNA repair and its therapeutic exploitation. British Journal of Cancer, 2011, 105, 1114–1122. [PubMed: 21989215]

(53). Hwang A; Maity A; McKenna WG; Muschel RJ Cell cycle-dependent regulation of the cyclin B1 promoter. The Journal of Biological Chemistry, 1995, 270, 28419–28424. [PubMed: 7499347]

(54). Stacey DW Cyclin D1 serves as a cell cycle regulatory switch in actively proliferating cells. Current Opinion in Cell Biology, 2003, 15, 158–163. [PubMed: 12648671]

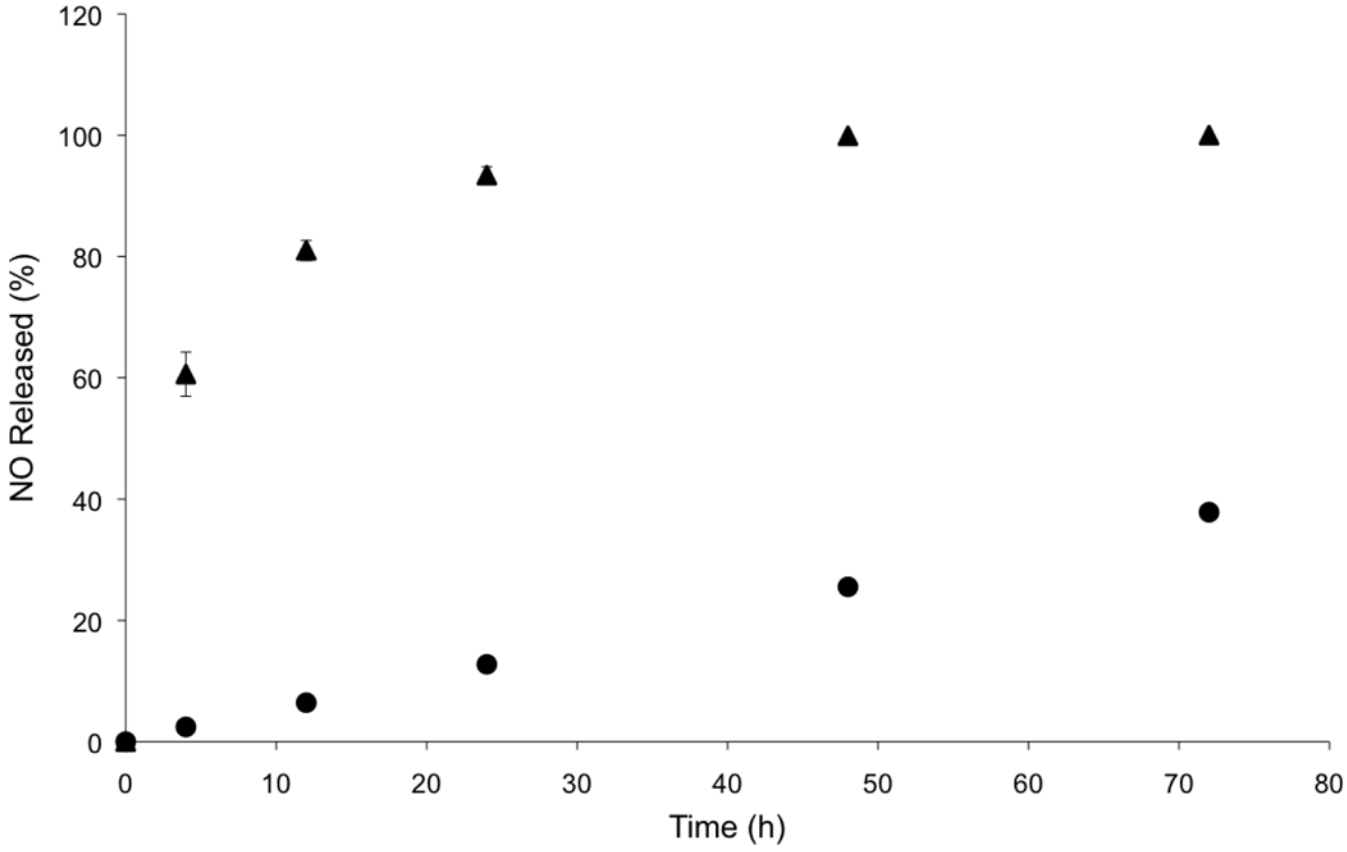

Figure 1.
Nitric oxide-release profiles from liposomal (●) DETA/NO and (▲) PAPA/NO in 10 mM PBS (pH 7.4, 37°C) over the first 72 h.

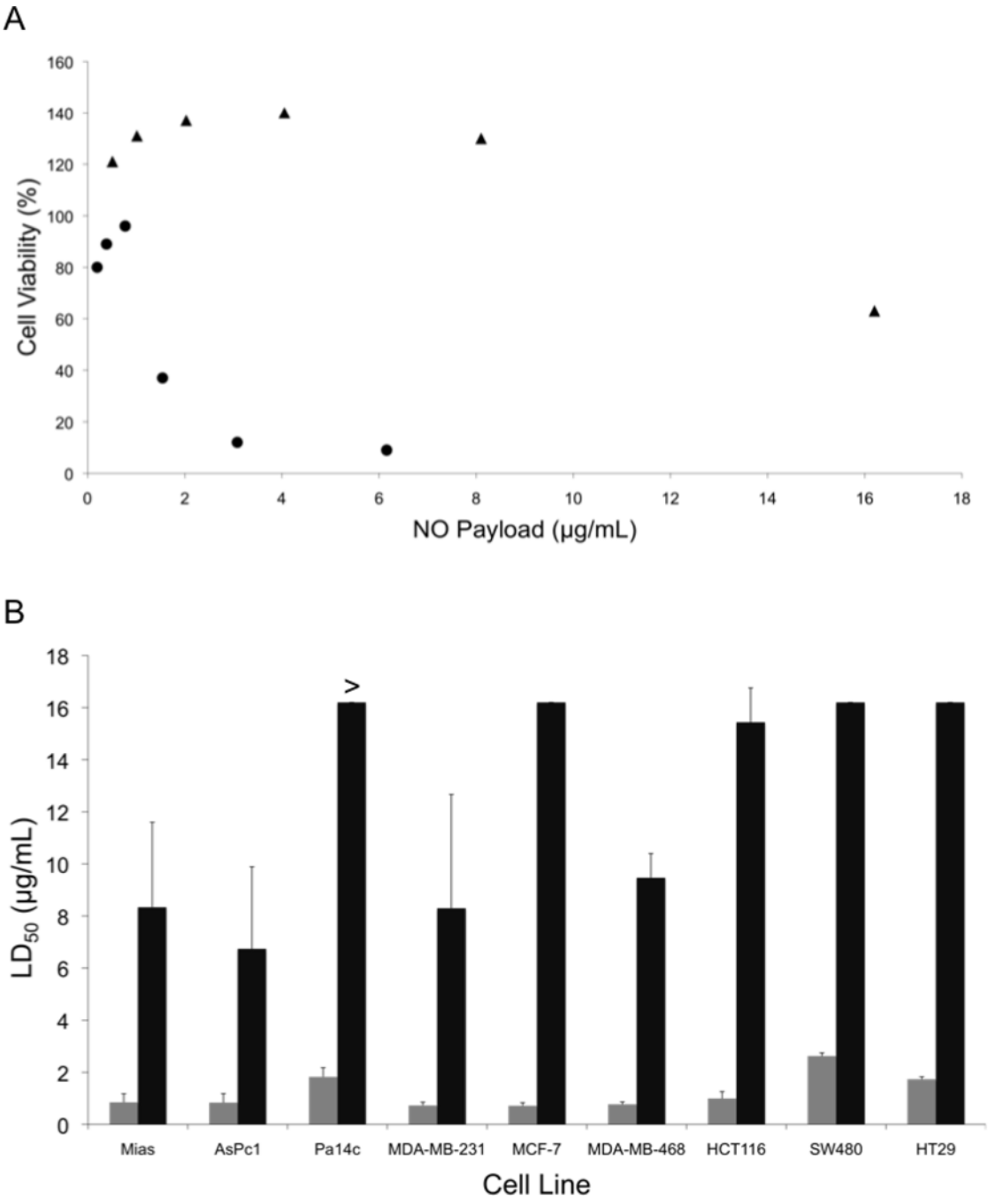

Figure 2.

(A) Cytotoxicity of liposomal (●) DETA/NO and (▲) PAPA/NO as a function of NO payload against human Pa14c pancreatic cancer cells after 72 h of exposure. (B) Calculated LD_{50} values for (grey bars) DETA/NO and (black bars) PAPA/NO liposomes against pancreatic, breast, and colorectal cancer cell lines. Of note, the LD_{50} of PAPA/NO liposomes against Pa14c cells was >16.2 μg/mL. NO payloads were calculated based on the total amount of NO released from the liposomes over 72 h in PBS.

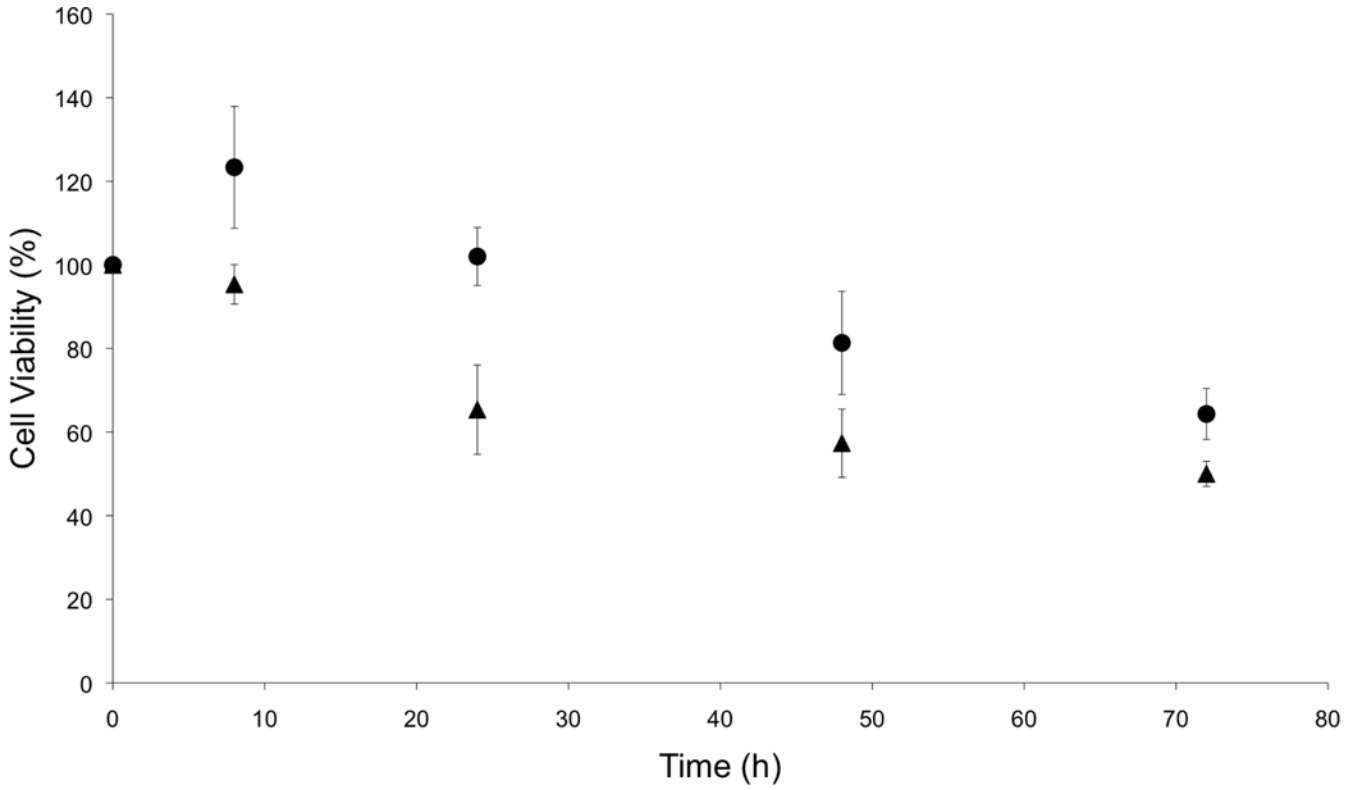

Figure 3.

Time-course cytotoxicity study of liposomal (●) DETA/NO and (▲) PAPA/NO at their respective LD_{50} values against human MCF-7 breast cancer cells.

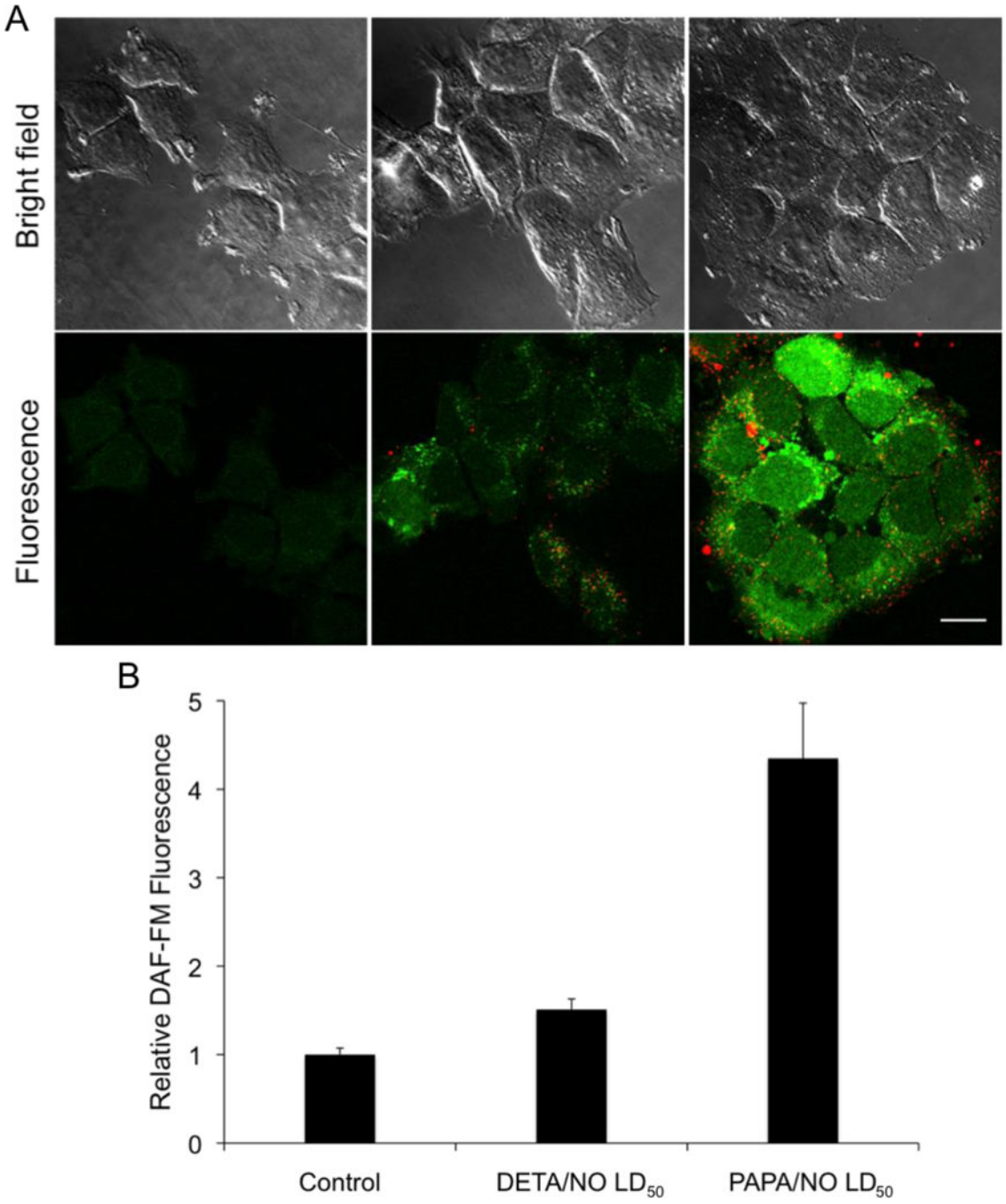

Figure 4.

(A) Confocal fluorescence images of MCF-7 cells incubated with DAF-FM (green) and treated with NO-releasing liposomes (red) for 2 h. Scale bar represents 15 μm. Column 1 is controls. Column 2 and 3 are cells exposed to the LD_{50} values of DETA/NO and PAPA/NO liposomes, respectively. By 2 h, DETA/NO and PAPA/NO liposomes released ~1 and 30% of their NO payloads, respectively. (B) Densitometric analysis of intracellular DAF-FM levels relative to untreated controls.

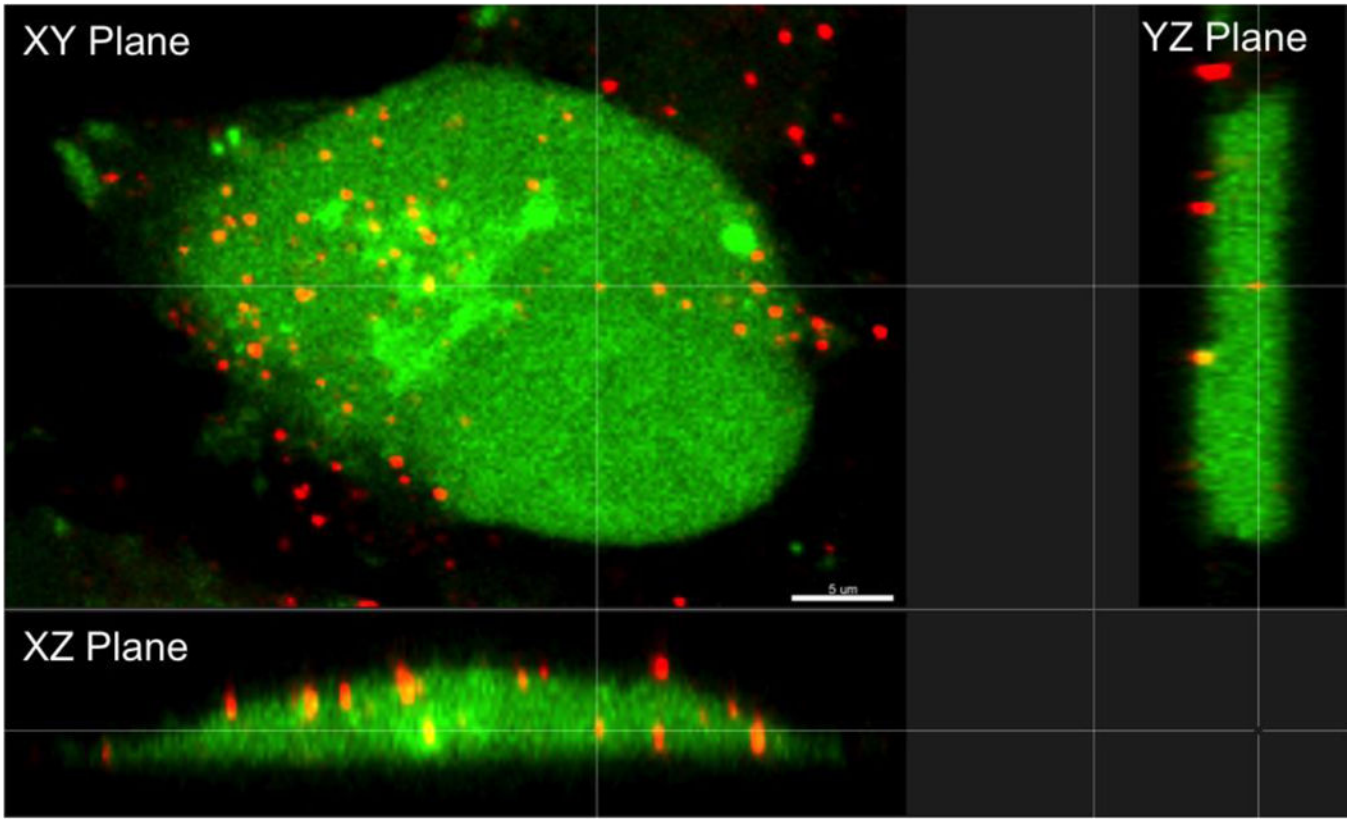

Figure 5.
Orthogonal view of MCF-7 cells after treatment with PAPA/NO liposomes. Scale bar represents 5 μm.

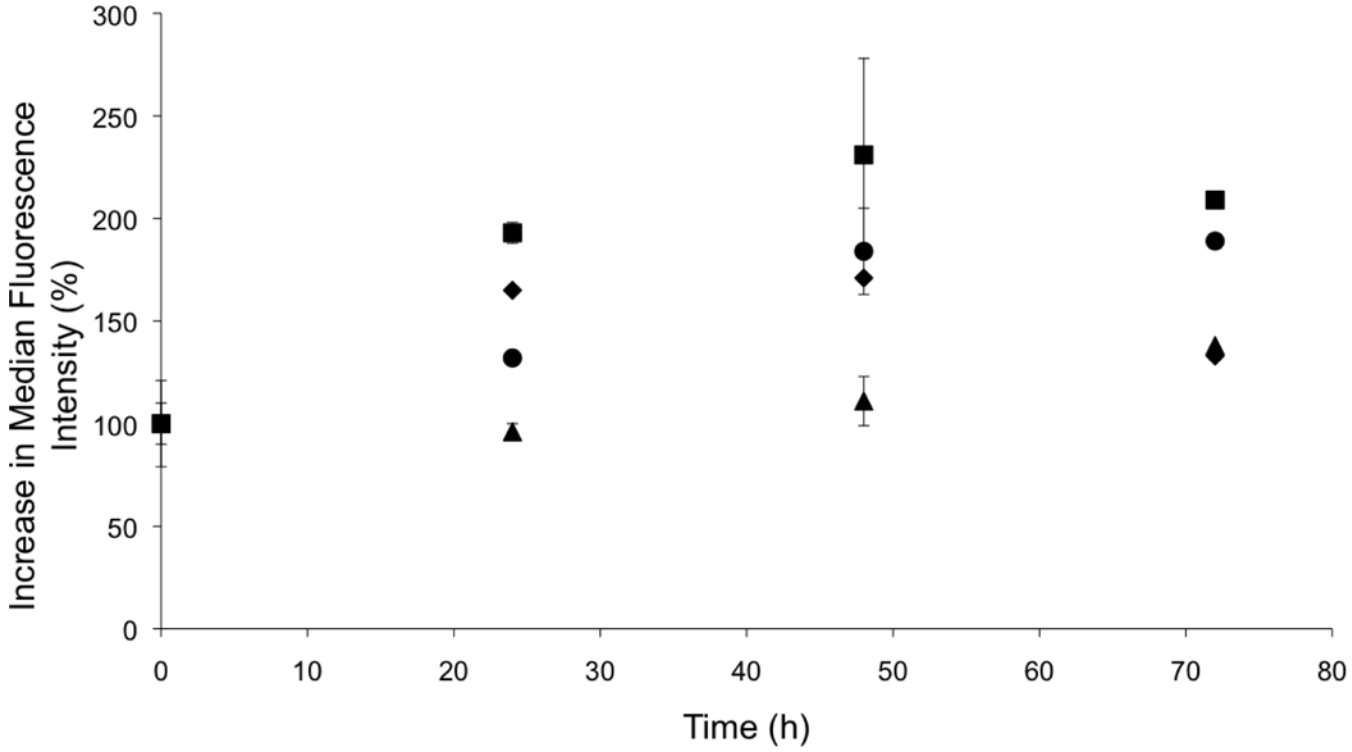

Figure 6.

Change in median fluorescence intensity over time indicating intracellular NO accumulation, as determined by flow cytometry, after treating MCF-7 cells with 0.75 μg/mL NO from (●) liposomal and (▲) free DETA/NO, and 16.2 μg/mL NO from (■) liposomal and (◆) free PAPA/NO.

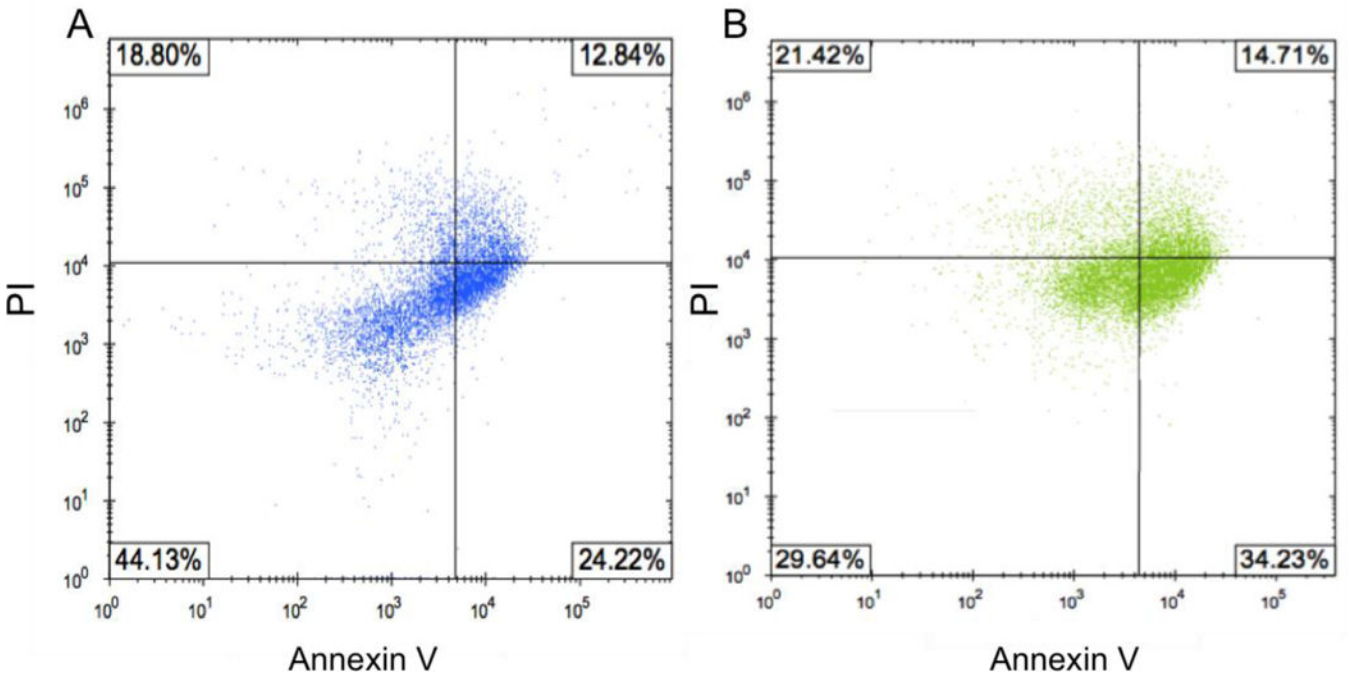

Figure 7.

Annexin V/PI quadrant plots for MCF-7 cells after 72 h exposure to (A) 16.2 μg/mL NO from PAPA/NO liposomes and (B) 0.75 μg/mL NO from DETA/NO liposomes (i.e., LD_{50} values). The percentages indicate the number of cells present in each quadrant. Units on axes are fluorescence intensities.

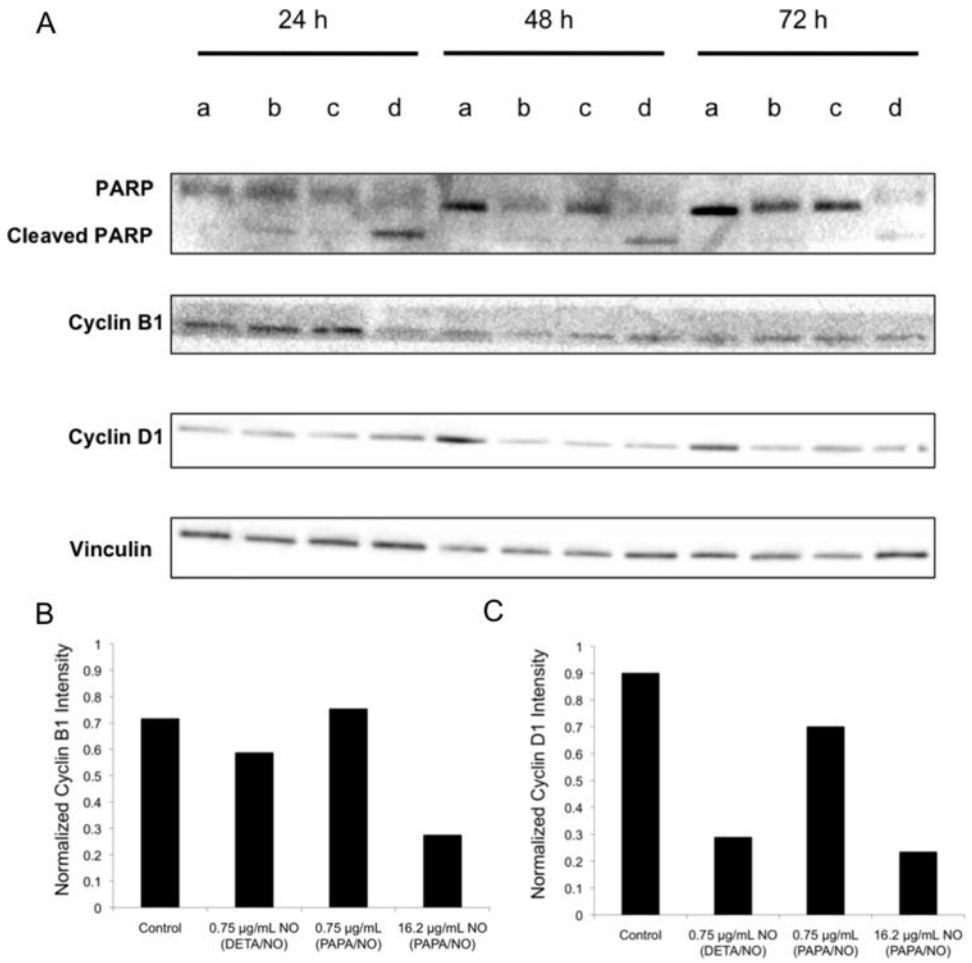

Figure 8.

(A) Western blot of MCF-7 cells after no treatment (lane a), 0.75 μg/mL NO from DETA/NO liposomes (lane b), 0.75 μg/mL NO from PAPA/NO liposomes (lane c), and 16.2 μg/mL NO from PAPA/NO liposomes (lane d). (B) Densitometric analysis of cyclin B1 levels after 24 h exposure. (C) Densitometric analysis of cyclin D1 levels after 72 h exposure.

Table 1.

Properties of NO-releasing liposomes.

NO Donor	Hydrodynamic size [a] (nm)	Encapsulation efficiency [b] (%)	Total NO[c] (μg/mL)
PAPA/NO	377 ± 52	19.0 ± 3.5	125.7 ± 41.1
DETA/NO	246 ± 32	20.6 ± 3.2	133.2 ± 26.7

[a] Z-average size measured using DLS.

[b] Ratio of μmol of NO inside liposomes to μmol used for synthesis, multiplied by 100.

[c] Total amount of NO released in acid normalized to the injected liposome volume.